Supplement of Atmos. Chem. Phys., 21, 11353–11378, 2021
https://doi.org/10.5194/acp-21-11353-2021-supplement

Atmospheric Chemistry and Physics
Open Access
EGU

Supplement of

Source apportionment of atmospheric PM_{10} oxidative potential: synthesis of 15 year-round urban datasets in France

Samuël Weber et al.

Correspondence to: Gaëlle Uzu (gaelle.uzu@ird.fr) and Samuël Weber (samuel.weber@univ-grenoble-alpes.fr)

Supplementary information

Contents

1 Interactive visualization website

Most of the data presented in this article can be interactively browsed at http://getopstandop.u-ga.fr, including timeserie, sources chemical profile determined by the PMF, etc. Each item can be found either by browsing the website, or refering to the list below :

- Input PMF and OP measurment:
  - Individual time series of OP and PMF factor contributions
    → http://getopstandop.u-ga.fr/results?component=rd_ts
  - Monthly aggregated view of measurments
    → http://getopstandop.u-ga.fr/results?component=rd_monthly
  - Seasonal aggregated view of measurments
    → http://getopstandop.u-ga.fr/results?component=rd_seasonal
- PMF analysis details
  - PMF profiles (absolute and relative chemical composition) and contributions to PM_{10}
    → http://getopstandop.u-ga.fr/results?component=pmf_profile_and_contribution
  - Chemical profile variability of the chemical composition of the PMF factor (absolute and relative composition) for each species
    → http://getopstandop.u-ga.fr/results?component=pmf_profiles
  - Similarity plot (PD-SID) of the chemical profiles
    → http://getopstandop.u-ga.fr/results?component=pmf_deltatool
  - Uncertainties from bootstrap and displacment for each PMF analysis
    → http://getopstandop.u-ga.fr/results?component=pmf_unc
  - Repartition of species among the differents PMF factors for each PMF analysis.
    → http://getopstandop.u-ga.fr/results?component=pmf_speciesrepartition
- Source apportionment of OP
  - Fit between the measured and modelled OP given by the MLR, together with the residuals.
    → http://getopstandop.u-ga.fr/results?component=op_obsvsmodel
  - Intrinsic OP from the MLR at each site (mean and standard deviation)
    → http://getopstandop.u-ga.fr/results?component=op_beta
  - Daily or seasonal mean and median contribution of the sources to the OP
    → http://getopstandop.u-ga.fr/results?component=op_contrib
  - Time serie of the source contributions to the OP, with the observed OP superimposed.
    → http://getopstandop.u-ga.fr/results?component=op_contrib_ts

2 Sampling sites description

Table S1 and Figure S1 describe the different sites and sampling periods used for this study. All PMF were run following the SOURCES program. PMF from Mobil'Air and DECOMBIO were re-run accordingly.

Table S1: Sampling sites meta-data.

Ville	Abbr.	Typology	Coordinate	m.a.s.l	# sample	Date	Research project
Marseille	MRS-5av	Urban bgd	43.3060 °N, 5.3957 °E	64	72	2015-01-11 → 2015-12-28	SOURCES[a]
Port-de-Bouc	PdB	Industrial	43.4019 °N, 4.9819 °E	1	113	2014-06-01 → 2015-05-17	SOURCES[a]
Aix-en-provence	AIX	Urban bgd	43.5302 °N, 5.4413 °E	188	56	2013-08-02 → 2014-07-13	SOURCES[a]
Nice	NIC	Urban traffic	43.7020 °N, 7.2862 °E	1	105	2014-07-11 → 2015-05-26	SOURCES[a]
Talence	TAL	Urban bgd	44.8004 °N, 0.5880 °W	20	120	2012-03-01 → 2013-03-19	SOURCES[a]
Nogent	NGT	Urban bgd	49.2763 °N, 2.4821 °E	28	135	2013-01-02 → 2014-05-11	SOURCES[a]
Grenoble	GRE-fr 2013	Urban bgd	45.1618 °N, 5.7356 °E	214	225	2013-01-02 → 2014-12-29	SOURCES[a]
Grenoble	GRE-fr 2017	Urban bgd	45.1618 °N, 5.7356 °E	214	122	2017-02-28 → 2018-03-10	Mobil'Air[b]
Grenoble	GRE-cb	Urban bgd	45.1833 °N, 5.7251 °E	212	124	2017-02-28 → 2018-03-10	Mobil'Air[b]
Vif	VIF	Urban bgd	45.0580 °N, 5.6768 °E	310	125	2017-02-28 → 2018-03-10	Mobil'Air[b]
Chamonix	CHAM	Urban valley	45.9225 °N, 6.8699 °E	1038	93	2013-11-02 → 2014-10-31	DECOMBIO[c]
Marnaz	MNZ	Urban valley	46.0577 °N, 6.5334 °E	504	89	2013-11-02 → 2014-10-31	DECOMBIO[c]
Passy	PAS	Urban valley	45.9235 °N, 6.7136 °E	588	88	2013-11-02 → 2014-10-31	DECOMBIO[c]
Roubaix	RBX	Traffic	50.7065 °N, 3.1806 °E	10	157	2013-01-20 → 2014-05-26	SOURCES[a]
Strasbourg	STG-cle	Traffic	48.5903 °N, 7.7450 °E	139	76	2013-04-11 → 2014-04-08	SOURCES[a]

m.a.s.l: meter after sea level (elevation)
Urban bgd: Urban background
[a] SOURCES program description by Weber et al. (2019)
[b] Mobil'Air program description by Borlaza et al. (2020)
[c] DECOMBIO program description by Chevrier (2016)

MRS-5av Marseille is a coastal and harbor city, and the second largest city in France. Its metropolitan area cover more than 3000 km² with more than 3 millions inhabitants.

PdB Port-de-Bouc is a small but heavily industrialized harbor city, near the "Étang de berre". The Étang de berre is the most important site for oil refinery in France, with lots of petroleum activities and ship traffic. Nearby, the Camargue salt marsh and Camargue regional park are also within 20 km of the station.

AIX Aix-en-provence is 20 km north of Marseille and the Étang de berre. Two main highways are deserving the city.

NIC The Nice city is populated by 1 million inhabitants. The harbor is mainly used by ferries joining the Corse or as marina. An important highway go around Nice and join Italy and France.

TAL Talence is located within the metropolitan area of Bordeauxi (more than 1 million inhabitants), 20 km east of the Atlantic ocean. Some industrial activity (pneumatic, refinnery or naval industry) are also present in the metropolitan area.

NGT Nogent-sur-oise is located 50 km north of Paris and is a city included within a conurbation of more than 85 000 inhabitants.

GRE-fr Urban background site of Grenoble. The Grenoble bassin is surrounded by 3 mountains ranges (Chartreuse, Vercors and Belledone) with frequent thermal inversion during winter. The station is located within a parc.

GRE-cb Urban hypercenter site in Grenoble, in a pedestrian area and a parc, but also urban road with frequent traffic jam during commuting.

VIF Peri-urban site 15 km away the main metropolitan area of Grenoble, near the Vercors regional parc. An important chemical industries complexe are within 10 km.

CHAM Urban site located in a narrow alpine valley (5 km large), near the Mont-Blanc mountain. A highway joining France and Italie with truck traffic pass in the Arve Valley, where lie Chamonix.

MNZ Urban site located in a narrow alpine valley (5 km large). An ski factory is implemented nearby. A highway joining France and Italie with truck traffic pass in the Arve Valley, where lies Marnaz.

PAS Urban site located in a narrow alpine valley (5 km large) A highway joining France and Italie with truck traffic pass in the Arve Valley, where lies Passy.

RBX Roubaix is located within the Lille metropolitan (second largest one) area in northern France, near the Belgium. The sampling station is a traffic site, located alongside an important highway.

STG-cle The Strasbourg conurbation represents 500000 inhabitants and is located at the frontier of France and Germany. The sampling station is a traffic site, located alongside an important highway.

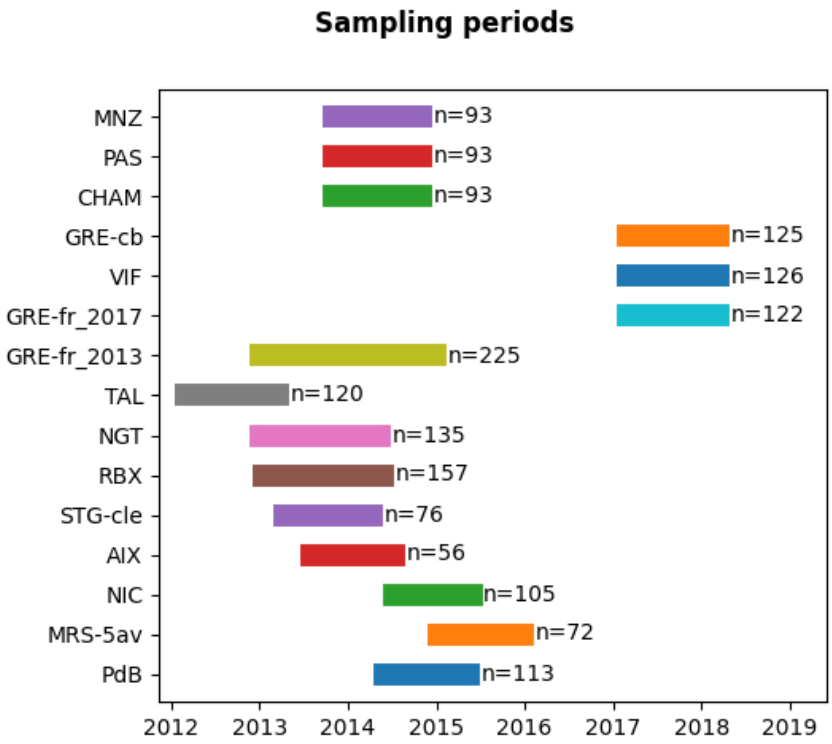

Figure S1: Sampling period and number of samples used per site in this study.

3 Input species for the PMF

The Table S2 below summarizes the input species used for each site. Due to the different sampling programs, the exact set of chemical species is not strictly identical at each site. Also, some species displaying lots of values lower than the quantification limit (QL) at some site, hence were removed from the PMF analysis.

Table S2: Species used as input for the different PMF runs.

specie	AIX	CHAM	GRE-cb	GRE-fr 2013	GRE-fr 2017	MNZ	MRS-5av	NGT	NIC	PAS	PdB	RBX	STG-cle	TAL	VIF
PM10	X	X	X	X	X	X	X	X	X	X	X	X	X	X	X
OC*	X	X	X	X	X	X	X	X	X	X	X	X	X	X	X
EC	X	X	X	X	X	X	X	X	X	X	X	X	X	X	X
Cl^-	X	X	X	X	X	X	X	X	X		X	X	X	X	X
NO_3^-	X	X	X	X	X	X	X	X	X	X	X	X	X	X	X
SO_4^{2-}	X	X	X	X	X	X	X	X	X	X	X	X	X	X	X
Na^+	X	X	X	X	X	X	X	X	X	X	X	X	X	X	X
NH_4^+	X	X	X	X	X	X	X	X	X	X	X	X	X	X	X
K^+	X	X	X	X	X	X	X	X	X	X	X	X	X	X	X
Mg^{2+}	X	X	X	X	X	X	X	X	X	X	X	X	X	X	X
Ca^{2+}	X	X	X	X	X	X	X	X	X	X	X	X	X	X	X
MSA	X	X	X	X	X	X	X	X	X	X	X	X	X	X	X
Levoglucosan	X	X	X	X	X	X	X	X	X	X	X	X	X	X	X
Mannosan	X	X	X	X	X	X	X	X	X	X	X	X	X	X	X
Polyols	X	X	X	X	X	X	X	X	X	X	X	X	X	X	X
Al			X	X	X	X				X	X	X	X		X
As	X	X	X		X	X	X	X	X	X	X	X	X	X	X
Ba	X	X				X	X	X	X	X	X	X	X	X	
Cd	X	X	X	X	X	X	X	X	X	X	X	X	X	X	X
Ce						X				X					
Co				X		X		X	X	X	X	X	X	X	
Cr	X	X	X		X	X	X		X	X	X		X		X
Cs				X							X	X	X		
Cu	X	X	X	X	X	X	X	X	X	X	X	X	X	X	X
Fe	X	X	X	X	X	X	X	X	X	X	X	X	X	X	X
La	X			X		X	X	X		X		X	X		
Li						X				X					
Mn	X	X	X	X	X	X	X	X	X	X	X	X	X	X	X
Mo	X	X	X	X	X	X	X	X	X	X		X	X	X	X
Ni	X	X	X	X	X	X	X	X	X	X	X	X	X	X	X
Pb	X	X	X	X	X	X	X	X	X	X	X	X	X	X	X
Rb	X	X	X	X	X	X	X	X		X	X	X	X		X
Sb	X	X	X	X	X	X		X	X	X	X	X	X	X	X
Se	X		X	X	X	X			X	X	X	X	X	X	X
Sn	X	X	X	X	X	X			X	X	X		X	X	X
Sr	X	X		X		X	X	X	X	X	X	X	X	X	
Ti	X	X	X		X	X	X		X	X	X	X	X	X	X
Tl										X					
V	X	X	X	X	X	X	X	X	X	X	X		X	X	X
Zn	X	X	X	X	X	X	X	X	X	X	X	X	X	X	X
Zr						X									

4 Determined PMF factors per site

Between 8 to 10 factors were successfully identified at each site. However, some of them were found only at some site. The determined PMF factor at each site are given in the Table S3. The common factors are Biomass burning, Nitrate rich, Primary biogenic, MSA rich, Road traffic, Sulfate rich and Aged salt. Some other factors reflect the specificity of the site typology, typically Heavy fuel oil (HFO) or industrial factors.

Table S3: PMF factors identified at each site.

Factor	Site															Identified	
	AIX	CHAM	GRE-cb	GRE-fr 2013	GRE-fr 2017	MNZ	MRS-5av	NGT	NIC	PAS	PdB	RBX	STG-cle	TAL	VIF	#	%
Aged salt	x		x	x	x		x	x	x		x	x	x	x	x	12	80%
Biomass burning	x	x	x	x	x	x	x	x	x	x	x	x	x	x	x	15	100%
Cadmium rich										x						1	7%
Dust	x	x	x	x	x	x	x		x	x	x	x		x	x	13	87%
HFO							x				x					2	13%
Industrial	x		x		x						x			x	x	6	40%
MSA rich	x	x	x	x	x	x	x	x		x	x	x	x	x	x	14	93%
Marine/HFO	x								x					x		3	20%
Nitrate rich	x	x	x	x	x	x	x	x	x	x	x	x	x	x	x	15	100%
Primary biogenic	x	x	x	x	x	x	x	x	x	x	x	x	x	x	x	15	100%
Resuspended dust													x			1	7%
Road traffic	x	x	x	x	x	x	x	x	x	x		x	x	x	x	14	93%
Salt	x	x					x	x	x		x	x		x		8	53%
Sea-road salt			x		x	x				x					x	5	33%
Sulfate rich		x	x	x	x	x	x	x	x	x	x	x	x		x	13	87%
Vanadium rich						x										1	7%
# factor	10	8	10	8	10	9	10	8	9	9	10	9	8	10	10		

5 Chemical profiles similarity

Similarity metrics used to assess the consistency of the PM factors' chemical profiles (PD: Pearson distance and SID: standardized identity distance defined in Pernigotti and Belis (2018)) are reported in Figure S2 for all the identified profiles. The figure reports the mean and standard deviation of the PD and SID for all possible pairs of profile but the details for each given pair of profile may be found in the website. According to Pernigotti and Belis (2018), two profiles are considered similar if their PD and SID fall down in the green rectangle delineating the area with PD<0.4 and SID<1.

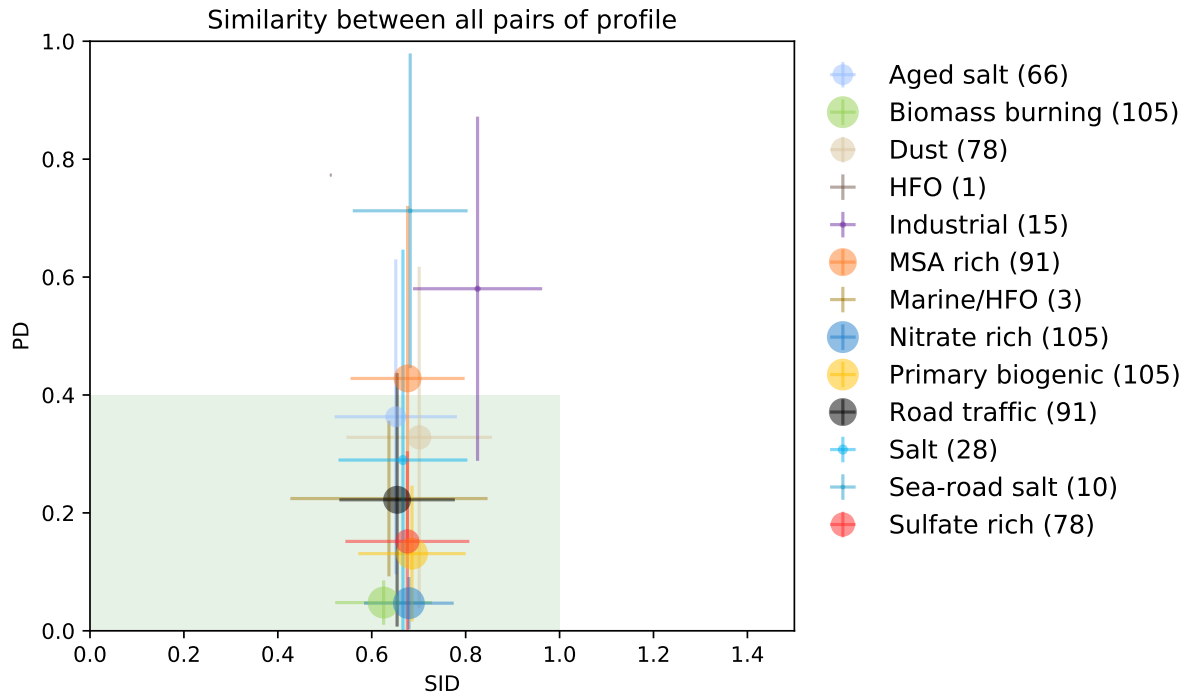

Figure S2: Similarity profile in the PD-SID space for all the pairs of PMF profile identified at all sites (see text for explanation). The mean (dot) and standard deviation (lines) are reported in the figure. The values in parenthesis indicate the number of pairs of profile considered: with $\binom{N}{2}$ the number of site where the profile is identified.

6 Accuracy of the different MLR

The accurary of the models is estimated by the regression between the observed OP_v and the one reconstructed by the MLR. In Table S4 is presented the regression line between observed (noted y) and reconstructed (noted $\hat{y}$), together with the Pearson correlation coefficient.

All scatter plots together with the residual plots can be found at http://getopstandop.u-ga.fr/results?component=op_obsvsmodel.

Table S4: Observed vs reconstructed OP equation and Pearson correlation, taking the mean value of the 500 bootstraps, for all the sites.

Site	OP^{DTT}		OP^{AA}	
	$y_{DTT} = a \times \hat{y}_{DTT} + b$	r^2	$y_{AA} = a \times \hat{y}_{AA} + b$	r^2
MRS-5av	$0.77 \times \hat{y} + 0.60$	0.72	$0.69 \times \hat{y} + 0.10$	0.72
PdB	$0.87 \times \hat{y} + 0.24$	0.84	$0.91 \times \hat{y} + 0.07$	0.87
AIX	$0.91 \times \hat{y} + 0.18$	0.82	$1.01 \times \hat{y} + 0.04$	0.92
NIC	$0.76 \times \hat{y} + 0.52$	0.79	$0.88 \times \hat{y} + 0.12$	0.83
TAL	$0.76 \times \hat{y} + 0.34$	0.77	$0.83 \times \hat{y} + 0.07$	0.86
NGT	$0.81 \times \hat{y} + 0.43$	0.75	$0.97 \times \hat{y} + 0.05$	0.87
GRE-fr 2013	$0.97 \times \hat{y} - 0.14$	0.79	$0.69 \times \hat{y} + 0.20$	0.79
GRE-fr 2017	$0.77 \times \hat{y} + 0.20$	0.81	$1.02 \times \hat{y} + 0.01$	0.94
GRE-cb	$0.70 \times \hat{y} + 0.35$	0.72	$0.81 \times \hat{y} + 0.20$	0.86
VIF	$0.62 \times \hat{y} + 0.47$	0.49	$0.78 \times \hat{y} + 0.20$	0.93
CHAM	$0.87 \times \hat{y} + 0.21$	0.90	$0.85 \times \hat{y} + 0.14$	0.93
MNZ	$0.87 \times \hat{y} + 0.19$	0.95	$0.90 \times \hat{y} - 0.01$	0.96
PAS	$0.76 \times \hat{y} + 0.72$	0.90	$0.96 \times \hat{y} - 0.06$	0.82
RBX	$0.75 \times \hat{y} + 0.49$	0.72	$0.86 \times \hat{y} + 0.31$	0.75
STG-cle	$0.75 \times \hat{y} + 0.57$	0.73	$0.55 \times \hat{y} + 0.64$	0.46

7 Intrinsic OP for the 8 main PM sources

The Table S5 presents the intrinsic OP (mean±standard deviation of the 500 bootstrap) in nmol min^{-1} $\mu\mathrm{g}^{-1}$ for the 8 main PMF factors. The first lines ("All") aggregated all the stations in a single mean and standard deviation value, plotted in the Figure 3 in the main text.

The Figure S3 represents the different intrisic OP distribution for the different sites in a comprehensive way.

Table S5: Mean and standard deviation of the regression coefficient (i.e. intrinsic OP) from the MLR for the 8 dominant sources in nmol min^{-1} $\mu\mathrm{g}^{-1}$.

	station	Aged salt	Biomass burning	Dust	MSA rich	Nitrate rich	Primary biogenic	Road traffic	Sulfate rich
DTT	All	0.038 ± 0.113	0.129 ± 0.065	0.121 ± 0.114	0.132 ± 0.410	0.044 ± 0.065	0.112 ± 0.113	0.223 ± 0.085	0.077 ± 0.082
	AIX	-0.134 ± 0.055	0.107 ± 0.028	0.224 ± 0.058	0.051 ± 0.063	0.015 ± 0.070	0.072 ± 0.072	0.200 ± 0.074	
	CHAM		0.092 ± 0.006	0.087 ± 0.018	0.240 ± 0.049	0.065 ± 0.028	0.131 ± 0.017	0.406 ± 0.060	0.082 ± 0.017
	GRE-cb	0.018 ± 0.046	0.105 ± 0.026	0.122 ± 0.021	0.779 ± 0.210	0.053 ± 0.021	0.282 ± 0.068	0.163 ± 0.042	-0.017 ± 0.033
	GRE-fr_{13}	0.181 ± 0.069	0.261 ± 0.022	0.131 ± 0.032	0.080 ± 0.136	-0.021 ± 0.060	0.165 ± 0.047	0.206 ± 0.033	0.186 ± 0.030
	GRE-fr_{17}	-0.083 ± 0.163	0.102 ± 0.047	0.094 ± 0.039	-0.173 ± 0.323	0.008 ± 0.018	0.237 ± 0.125	0.183 ± 0.038	0.054 ± 0.035
	MRS-5av	0.110 ± 0.044	0.114 ± 0.068	0.025 ± 0.022	0.168 ± 0.224	0.088 ± 0.102	-0.046 ± 0.090	0.243 ± 0.053	0.025 ± 0.035
	MNZ		0.116 ± 0.005	0.069 ± 0.015	0.095 ± 0.031	0.053 ± 0.007	0.071 ± 0.009	0.253 ± 0.018	0.086 ± 0.007
	NIC	0.120 ± 0.026	0.117 ± 0.013	0.110 ± 0.027		0.081 ± 0.046	0.004 ± 0.048	0.279 ± 0.084	0.082 ± 0.024
	NGT	0.116 ± 0.043	0.191 ± 0.035		0.533 ± 0.298	0.023 ± 0.035	-0.038 ± 0.114	0.159 ± 0.035	0.198 ± 0.046
	PAS		0.129 ± 0.011	0.109 ± 0.015	0.161 ± 0.075	0.161 ± 0.055	0.186 ± 0.031	0.256 ± 0.044	0.114 ± 0.021
	PdB	0.032 ± 0.032	0.179 ± 0.014	0.140 ± 0.019	0.123 ± 0.080	0.017 ± 0.022	0.161 ± 0.026		0.098 ± 0.035
	RBX	-0.006 ± 0.050	-0.018 ± 0.043	0.251 ± 0.016	-0.096 ± 0.072	0.066 ± 0.009	0.004 ± 0.042	0.189 ± 0.028	-0.106 ± 0.046
	STG-cle	0.137 ± 0.037	0.155 ± 0.017		0.370 ± 0.071	0.084 ± 0.018	0.154 ± 0.035	0.197 ± 0.018	0.098 ± 0.021
	TAL	-0.044 ± 0.030	0.147 ± 0.019	0.103 ± 0.021	0.063 ± 0.043	-0.036 ± 0.032	0.142 ± 0.045	0.272 ± 0.096	
	VIF	0.004 ± 0.068	0.144 ± 0.028	0.105 ± 0.344	-0.540 ± 0.870	0.002 ± 0.019	0.148 ± 0.038	0.116 ± 0.032	0.106 ± 0.025
AA	All	0.024 ± 0.054	0.197 ± 0.103	0.037 ± 0.086	-0.020 ± 0.156	0.010 ± 0.056	0.028 ± 0.067	0.161 ± 0.108	0.009 ± 0.024
	AIX	-0.049 ± 0.046	0.194 ± 0.018	0.157 ± 0.027	0.051 ± 0.058	0.118 ± 0.082	0.030 ± 0.068	0.221 ± 0.068	
	CHAM		0.174 ± 0.012	-0.048 ± 0.015	0.001 ± 0.037	-0.032 ± 0.039	0.025 ± 0.015	0.297 ± 0.043	-0.011 ± 0.008
	GRE-cb	-0.007 ± 0.027	0.169 ± 0.036	-0.015 ± 0.016	-0.169 ± 0.103	0.030 ± 0.012	0.015 ± 0.038	0.196 ± 0.024	0.029 ± 0.010
	GRE-fr_{13}	0.037 ± 0.019	0.183 ± 0.011	0.012 ± 0.011	-0.036 ± 0.032	-0.004 ± 0.014	0.032 ± 0.014	0.129 ± 0.009	0.002 ± 0.013
	GRE-fr_{17}	0.103 ± 0.083	0.368 ± 0.026	0.017 ± 0.008	-0.016 ± 0.100	-0.036 ± 0.017	-0.010 ± 0.036	0.182 ± 0.020	0.042 ± 0.011
	MRS-5av	0.016 ± 0.007	0.101 ± 0.012	0.004 ± 0.007	-0.029 ± 0.034	0.004 ± 0.009	0.001 ± 0.018	0.023 ± 0.015	0.001 ± 0.006
	MNZ		0.266 ± 0.012	0.006 ± 0.011	0.082 ± 0.016	-0.084 ± 0.030	0.027 ± 0.009	0.154 ± 0.022	0.014 ± 0.009
	NIC	0.034 ± 0.022	0.112 ± 0.011	-0.001 ± 0.016		-0.018 ± 0.017	-0.034 ± 0.028	0.354 ± 0.047	0.013 ± 0.010
	NGT	0.069 ± 0.031	0.428 ± 0.060		-0.078 ± 0.234	0.063 ± 0.035	0.225 ± 0.095	0.074 ± 0.046	-0.016 ± 0.038
	PAS		0.161 ± 0.013	-0.002 ± 0.007	-0.013 ± 0.035	0.040 ± 0.058	0.007 ± 0.016	0.047 ± 0.023	-0.003 ± 0.015
	PdB	0.011 ± 0.014	0.138 ± 0.007	0.034 ± 0.008	-0.003 ± 0.026	-0.011 ± 0.015	0.035 ± 0.011		0.006 ± 0.008
	RBX	0.069 ± 0.026	0.223 ± 0.042	0.167 ± 0.023	0.090 ± 0.063	0.019 ± 0.012	0.036 ± 0.040	0.317 ± 0.039	0.028 ± 0.036
	STG-cle	-0.023 ± 0.030	0.026 ± 0.025		0.080 ± 0.020	0.044 ± 0.012	0.015 ± 0.025	0.128 ± 0.017	-0.007 ± 0.011
	TAL	0.008 ± 0.017	0.134 ± 0.015	0.006 ± 0.009	-0.015 ± 0.030	0.004 ± 0.010	0.004 ± 0.027	0.081 ± 0.051	
	VIF	0.021 ± 0.041	0.284 ± 0.023	0.150 ± 0.181	-0.221 ± 0.385	0.015 ± 0.020	0.014 ± 0.022	0.052 ± 0.015	0.021 ± 0.009

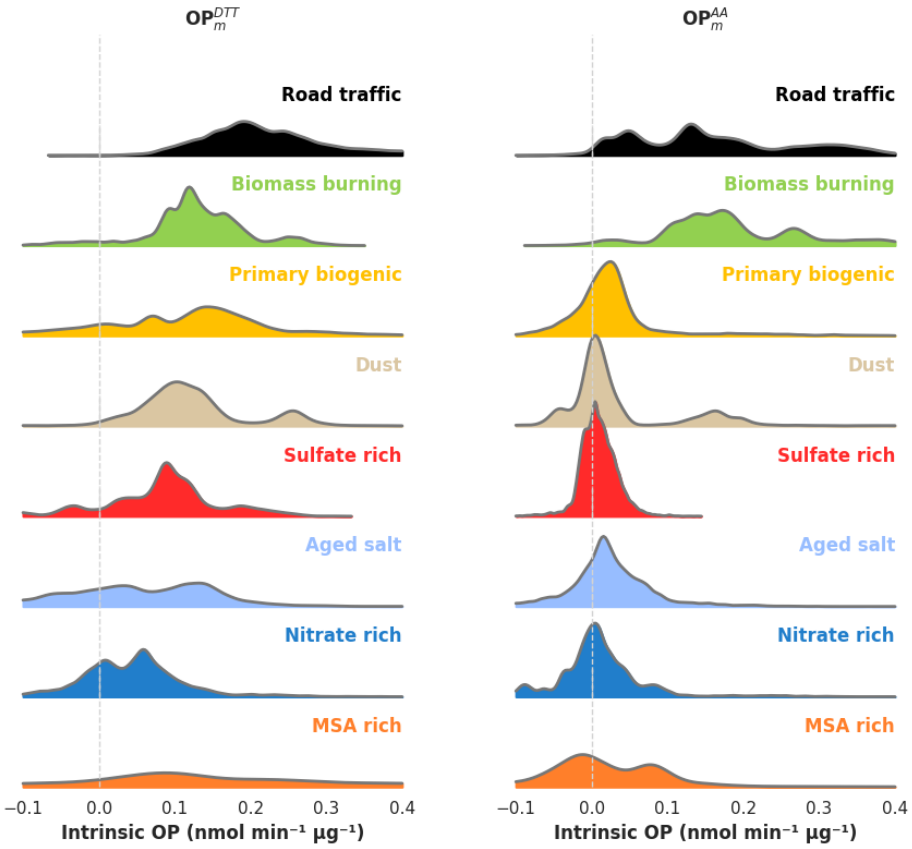

Figure S3: Kernel density representation of the different intrisinc OP obtained from the bootstraping method for all sites.

8 Intrinsic OP^{DTT} per station and all PMF factors

Details of the different regression coefficients (i.e. intrinsic OP) of the OP^{DTT} MLR for each site are presented in Table S6 in nmol min^{-1} μg^{-1} for the PMF profile and in nmol min^{-1} m^{-3} for the constant of the MLR. The results are the mean(1std) of the 500 bootstrap.

Table S6: Intrinsic OP^{DTT} of each PMF factor for the individual station (in nmol min^{-1} μg^{-1}) and constant (in nmol min^{-1} m^{-3}) from the MLR.

PMF profile	AIX	CHAM	GRE-cb	GRE-fr 2013	GRE-fr 2017	MNZ	MRS-5av	NGT	NIC	PAS	PdB	RBX	STG-cle	TAL	VIF
Aged salt	−0.134(55)		0.018(46)	0.181(69)	−0.083(163)		0.110(44)	0.116(43)	0.120(26)		0.032(32)	−0.006(50)	0.137(37)	−0.044(30)	0.004(68)
Biomass burning	0.107(28)	0.092(6)	0.105(26)	0.261(22)	0.102(47)	0.116(5)	0.114(68)	0.191(35)	0.117(13)	0.129(11)	0.179(14)	−0.018(43)	0.155(17)	0.147(19)	0.144(28)
Cadmium rich										0.244(482)					
Dust	0.224(58)	0.087(18)	0.122(21)	0.131(32)	0.094(39)	0.069(15)	0.025(22)		0.110(27)	0.109(15)	0.140(19)	0.251(16)		0.103(21)	0.105(344)
HFO							0.514(143)				0.216(42)				
Industrial	−0.023(92)		0.520(304)		0.371(268)						0.025(40)			0.079(55)	0.144(396)
MSA rich	0.051(63)	0.240(49)	0.779(210)	0.080(136)	−0.173(323)	0.095(31)	0.168(224)	0.533(298)		0.161(75)	0.123(80)	−0.096(72)	0.370(71)	0.063(43)	−0.540(870)
Marine/HFO	0.061(30)								0.040(29)					0.136(61)	
Nitrate rich	0.015(70)	0.065(28)	0.053(21)	−0.021(60)	0.008(18)	0.053(7)	0.088(102)	0.023(35)	0.081(46)	0.161(55)	0.017(22)	0.066(9)	0.084(18)	−0.036(32)	0.002(19)
Primary biogenic	0.072(72)	0.131(17)	0.282(68)	0.165(47)	0.237(125)	0.071(9)	−0.046(90)	−0.038(114)	0.004(48)	0.186(31)	0.161(26)	0.004(42)	0.154(35)	0.142(45)	0.148(38)
Resuspended dust													0.087(30)		
Road traffic	0.200(74)	0.406(60)	0.163(42)	0.206(33)	0.183(38)	0.253(18)	0.243(53)	0.159(35)	0.279(84)	0.256(44)		0.189(28)	0.197(18)	0.272(96)	0.116(32)
Salt	0.440(144)	0.117(26)					−0.200(124)	0.059(40)	0.115(52)		0.117(31)	0.000(49)		0.049(23)	
Sea-road salt			−0.098(82)		0.192(105)	−0.009(24)				0.000(192)					0.187(105)
Sulfate rich		0.082(17)	−0.017(33)	0.186(30)	0.054(35)	0.086(7)	0.025(35)	0.198(46)	0.082(24)	0.114(21)	0.098(35)	−0.106(46)	0.098(21)		0.106(25)
Vanadium rich						0.087(18)									
constante	0.186(210)	0.144(76)	0.120(102)	−0.526(131)	0.096(89)	0.024(49)	0.508(198)	0.052(189)	0.445(132)	−0.293(188)	−0.090(181)	0.861(274)	−0.148(147)	0.133(134)	−0.008(120)

9 Intrinsic OP^{AA} per station and all PMF factors

Details of the different regression coefficients (i.e. intrinsic OP) of the OP^{AA} MLR for each site are presented in Table S7 in nmol min^{-1} μg^{-1} for the PMF profile and in nmol min^{-1} m^{-3} for the constant of the MLR. The results are the mean(1std) of the 500 bootstrap.

Table S7: Intrinsic OP^{AA} of each PMF factor for the individual station (in nmol min^{-1} μg^{-1}) and constant (in nmol min^{-1} m^{-3}) from the MLR.

PMF profile	AIX	CHAM	GRE-cb	GRE-fr 2013	GRE-fr 2017	MNZ	MRS-5av	NGT	NIC	PAS	PdB	RBX	STG-cle	TAL	VIF
Aged salt	-0.049(46)		−0.007(27)	0.037(19)	0.103(83)		0.016(7)	0.069(31)	0.034(22)		0.011(14)	0.069(26)	−0.023(30)	0.008(17)	0.021(41)
Biomass burning	0.194(18)	0.174(12)	0.169(36)	0.183(11)	0.368(26)	0.266(12)	0.101(12)	0.428(60)	0.112(11)	0.161(13)	0.138(7)	0.223(42)	0.026(25)	0.134(15)	0.284(23)
Cadmium rich										0.440(299)					
Dust	0.157(27)	−0.048(15)	−0.015(16)	0.012(11)	0.017(8)	0.006(11)	0.004(7)		−0.001(16)	−0.002(7)	0.034(8)	0.167(23)		0.006(9)	0.150(181)
HFO							0.036(22)				0.109(27)				
Industrial	0.033(90)		0.825(295)		0.611(169)						0.014(17)			0.051(26)	0.099(297)
MSA rich	0.051(58)	0.001(37)	−0.169(103)	−0.036(32)	−0.016(100)	0.082(16)	−0.029(34)	−0.078(234)		−0.013(35)	−0.003(26)	0.090(63)	0.080(20)	−0.015(30)	−0.221(385)
Marine/HFO	-0.006(18)								−0.012(21)					−0.020(28)	
Nitrate rich	0.118(82)	−0.032(39)	0.030(12)	−0.004(14)	−0.036(17)	−0.084(30)	0.004(9)	0.063(35)	−0.018(17)	0.040(58)	−0.011(15)	0.019(12)	0.044(12)	0.004(10)	0.015(20)
Primary biogenic	0.030(68)	0.025(15)	0.015(38)	0.032(14)	−0.010(36)	0.027(9)	0.001(18)	0.225(95)	−0.034(28)	0.007(16)	0.035(11)	0.036(40)	0.015(25)	0.004(27)	0.014(22)
Resuspended dust													0.103(44)		
Road traffic	0.221(68)	0.297(43)	0.196(24)	0.129(9)	0.182(20)	0.154(22)	0.023(15)	0.074(46)	0.354(47)	0.047(23)		0.317(39)	0.128(17)	0.081(51)	0.052(15)
Salt	0.173(108)	0.139(23)					−0.008(27)	0.029(34)	0.043(22)		0.001(11)	0.119(26)		0.000(9)	
Sea-road salt			0.106(92)		0.042(42)	−0.042(35)				0.055(70)					0.157(134)
Sulfate rich		−0.011(8)	0.029(10)	0.002(13)	0.042(11)	0.014(9)	0.001(6)	−0.016(38)	0.013(10)	−0.003(15)	0.006(8)	0.028(36)	−0.007(11)		0.021(9)
Vanadium rich						0.014(14)									
const	-0.035(160)	0.236(72)	0.165(78)	0.042(55)	−0.041(62)	−0.053(80)	0.113(41)	−0.011(174)	0.000(73)	0.224(162)	−0.027(42)	−0.556(211)	0.396(106)	0.199(112)	0.110(87)

References

Borlaza, Lucille Joanna S., Samuël Weber, Gaëlle Uzu, Véronique Jacob, Trishalee Cañete, Olivier Favez, Steve Micallef, Cécile Trébuchon, Rémy Slama, and Jean-Luc Jaffrezo (Dec. 10, 2020). "Disparities in Particulate Matter (PM_{10}) Origins and Oxidative Potential at a City-Scale (Grenoble, France) – Part I: Source Apportionment at Three Neighbouring Sites". In: *Atmospheric Chemistry and Physics Discussions*, pp. 1–35. ISSN: 1680-7316. DOI: 10.5194/acp-2020-1144. URL: https://acp.copernicus.org/preprints/acp-2020-1144/ (visited on 12/11/2020).

Chevrier, Florie (2016). "Chauffage au bois et qualité de l'air en Vallée de l'Arve : définition d'un système de surveillance et impact d'une politique de rénovation du parc des appareils anciens." Grenoble: Université Grenoble Alpes. 218 pp. URL: https://tel.archives-ouvertes.fr/tel-01527559 (visited on 06/28/2018).

Pernigotti, Denise and Claudio A. Belis (May 2018). "DeltaSA Tool for Source Apportionment Benchmarking, Description and Sensitivity Analysis". In: *Atmospheric Environment* 180, pp. 138–148. ISSN: 13522310. DOI: 10.1016/j.atmosenv.2018.02.046. URL: http://linkinghub.elsevier.com/retrieve/pii/S1352231018301316 (visited on 06/14/2018).

Weber, Samuël, Dalia Salameh, Alexandre Albinet, Laurent Y. Alleman, Antoine Waked, Jean-Luc Besombes, Véronique Jacob, Géraldine Guillaud, Boualem Mesbah, Benoit Rocq, Agnès Hulin, Marta Dominik-Sègue, Eve Chrétien, Jean-Luc Jaffrezo, and Olivier Favez (June 2019). "Comparison of PM_{10} Sources Profiles at 15 French Sites Using a Harmonized Constrained Positive Matrix Factorization Approach". In: *Atmosphere* 10.6, p. 310. ISSN: 2073-4433. DOI: 10.3390/atmos10060310. URL: https://www.mdpi.com/2073-4433/10/6/310 (visited on 06/04/2019).